

NMR Chemical Shielding and Spin–Spin Coupling Constants of Liquid NH₃: A Systematic Investigation using the Sequential QM/MM Method[†]

Rodrigo M. Gester,[‡] Herbert C. Georg,^{‡,§} Sylvio Canuto,[‡] M. Cristina Caputo,^{*,||} and Patricio F. Provasi[†]

Instituto de Física, Universidade de São Paulo, CP 66318, 05315-970, São Paulo, SP, Brazil, Instituto de Física, Universidade Federal de Goiás, CP 131, 74001-970, Goiânia, GO, Brazil, Department of Physics, University of Buenos Aires, Ciudad Universitaria 1400 - Buenos Aires, Argentina, and I-MIT (CONICET) and Department of Physics, Northeastern University, Av. Libertad 5500, W 3404 AAS - Corrientes, Argentina

Received: May 29, 2009; Revised Manuscript Received: July 16, 2009

The NMR spin coupling parameters, $^1J(\text{N,H})$ and $^2J(\text{H,H})$, and the chemical shielding, $\sigma(^{15}\text{N})$, of liquid ammonia are studied from a combined and sequential QM/MM methodology. Monte Carlo simulations are performed to generate statistically uncorrelated configurations that are submitted to density functional theory calculations. Two different Lennard–Jones potentials are used in the liquid simulations. Electronic polarization is included in these two potentials via an iterative procedure with and without geometry relaxation, and the influence on the calculated properties are analyzed. B3LYP/aug-cc-pVTZ-J calculations were used to compute the $^1J(\text{N,H})$ constants in the interval of -67.8 to -63.9 Hz, depending on the theoretical model used. These can be compared with the experimental results of -61.6 Hz. For the $^2J(\text{H,H})$ coupling the theoretical results vary between -10.6 to -13.01 Hz. The indirect experimental result derived from partially deuterated liquid is -11.1 Hz. Inclusion of explicit hydrogen bonded molecules gives a small but important contribution. The vapor-to-liquid shifts are also considered. This shift is calculated to be negligible for $^1J(\text{N,H})$ in agreement with experiment. This is rationalized as a cancellation of the geometry relaxation and pure solvent effects. For the chemical shielding, $\sigma(^{15}\text{N})$ calculations at the B3LYP/aug-pcS-3 show that the vapor-to-liquid chemical shift requires the explicit use of solvent molecules. Considering only one ammonia molecule in an electrostatic embedding gives a wrong sign for the chemical shift that is corrected only with the use of explicit additional molecules. The best result calculated for the vapor to liquid chemical shift $\Delta\sigma(^{15}\text{N})$ is -25.2 ppm, in good agreement with the experimental value of -22.6 ppm.

1. Introduction

Nuclear magnetic resonance (NMR) is a very important technique for the characterization of molecules and biomolecules.¹ Most NMR measurements are made in liquids and the environment influences the NMR parameters compared to the free molecule (corresponding to a gas phase). In recent years theoretical methods devoted to the description of solvent effects^{2,3} have also directed attention to the importance of understanding the solvent effects on the NMR constants.^{4–6} Essentially two major theoretical lines are used. On one side, the so-called continuum methods,² which are a sophisticated extension of the original ideas of Onsager⁷ and Kirkwood,⁸ have been used with relative success. On the other side, there are fast developments and applications of discrete methods where the statistical nature of the liquid is considered.⁹ Several previous studies have been made where the solvent effects on NMR parameters are considered. Normally this is done considering a reference molecule in a given solvent. We are now interested in the theoretical description of the NMR parameters of homogeneous liquids. In addition, NMR for nitrogen atoms ^{15}N has seen an increasing interest.^{5,10} We will consider liquid ammonia where the vapor–liquid chemical shift of the $\sigma(^{15}\text{N})$

parameter has been obtained experimentally with good accuracy. Also, the intramolecular spin–spin coupling constants (SSCC), $^1J(^{15}\text{N},^1\text{H})$, and $^2J(^1\text{H},^1\text{H})$ are of considerable interest^{11–17} and will be calculated here.

Measurement of the SSCC of ammonia were first made by Bernheim and Batiz-Hernandez¹¹ in a liquid mixture of $^{15}\text{NH}_3$, $^{15}\text{NH}_2\text{D}$, $^{15}\text{NHD}_2$, and $^{15}\text{ND}_3$. They reported an averaged one-bond coupling $^1J(\text{N,H})$ value of -61.2 ± 0.9 Hz and a two-bond coupling $^2J(\text{H,H})$ of -10.35 ± 0.80 Hz. As it is well-known, this value cannot be directly measured in NH_3 because the three protons are chemical and magnetically equivalent, but it is derived from the H–D coupling in partially deuterated ammonia, via $^2J(\text{H,H}) = (\gamma_{\text{H}}/\gamma_{\text{D}})^2J(\text{D,H})$. No deuterium effect was obtained, that is, within the experimental error they find¹¹ that the values of $^{15}\text{NH}_2\text{D}$ and $^{15}\text{NHD}_2$ are the same. Next, Alei, Jr. et al.¹² reported the value of -61.2 ± 0.3 Hz for the $^1J(\text{N,H})$ parameter of vapor ammonia. Later, Wasylishen and Friedrich¹² made higher accuracy experiments to obtain the deuterium isotope effect on the nuclear shielding and the SSCC of ammonia. They reported, the following values of the one-bond coupling $^1J(\text{N,H})$: -61.45 Hz for NH_3 , -61.38 Hz for NH_2D , and -61.31 Hz for NHD_2 ; and the following ones for the stretched one-bond couplings $^1J(\text{N,D})(\gamma_{\text{H}}/\gamma_{\text{D}})$: -61.85 Hz for NH_2D_1 , -61.77 Hz for NH_1D_2 and -61.69 Hz for ND_3 with an error of ± 0.13 Hz. The deuterium isotope effect yields an increase of the $^1J(\text{N,H})$ spin coupling of about 0.07 Hz for each

[†] Part of the “Vincenzo Aquilanti Festschrift”.

* Corresponding author.

[‡] Universidade de São Paulo.

[§] Universidade Federal de Goiás.

^{||} University of Buenos Aires.

[†] Northeastern University.

substituted hydrogen. For the two-bond coupling ${}^2J(\text{H,H})$, Wasylishen and Friedrich reported a value of ${}^2J(\text{H,H})$ of -9.6 ± 0.2 Hz.

Jameson et al.¹⁷ have also studied the NMR properties of NH₃ and reported^{17b} the gas phase value of ${}^1J(\text{N-H})$ as -61.7 ± 0.2 Hz and compared with the liquid value of -61.8 ± 0.5 Hz obtained by Lichtman et al.^{16a} These results and also those obtained independently in refs 11–13 indicate that the vapor to liquid shift ${}^1J(\text{N-H})$ is negligible, or considering the experimental errors, less than 0.8 Hz. The physical origin of this small shift deserves a theoretical analysis.

The chemical shielding, $\sigma({}^{15}\text{N})$, presents a more pronounced dependence of the vapor to liquid chemical shift. The first experimental determination of $\sigma({}^{15}\text{N})$ in ammonia was made by Litchman et al.,^{16a} who reported a shift of -22.6 ± 0.2 ppm from gas to liquid phase, at 195.5 K.

Theoretical predictions of both couplings, ${}^1J(\text{N,H})$ and ${}^2J(\text{H,H})$, were made by different authors, but probably the first one was made by Berthier and Berthier¹² at the Hartree–Fock level. However, many other estimates appeared later in the literature.¹⁵ Among these an interesting study was made by Ruden et al., ref 15g, where they estimated at the B3LYP/sHIII level of theory the zero-point vibrational correction to ${}^1J(\text{N,H})$ and ${}^2J(\text{H,H})$ to be 0.4 and 0.7 Hz, respectively. Then, subtracting these corrections to the experiments they obtained the empirically zero point corrected values of ${}^2J(\text{N,H}) = -61.9$ Hz and ${}^2J(\text{H,H}) = -10.3$ Hz. These are close to the inferred indirect experimental values of Bernheim and Batiz-Hernandez.¹¹

In this work we focus on a detailed and systematic investigation of the NMR parameters of NH₃ with explicit consideration of the liquid nature of the system. We use a combined and sequential QM/MM method.¹⁸ The structure of liquid NH₃ is generated by classical Monte Carlo (MC) simulation. Two different force fields are used. Electronic polarization is considered taking into account the changes in the electrostatic moments of NH₃ when in the liquid phase. Similarly, geometry relaxation of ammonia in the liquid is considered and its role is analyzed.

This paper is organized as follows. In section 2 we introduce the theoretical details of the Monte Carlo simulation and the iterative procedure for obtaining the electronic polarization and the quantum mechanical methods for the calculations of the magnetic properties. Section 3.1 discusses the results at different levels of approximation for the electronic polarization and the corresponding in-liquid dipole moments and geometries. Section 3.2 presents in detail our calculations for the intramolecular spin–spin coupling and the solvent effects with comparison to experimental results. Section 3.3 is devoted to solvent effects on the ${}^{15}\text{N}$ chemical shielding, systematically analyzing the separate theoretical contributions and their level of agreement with measurements. Finally, in section 4 we summarize our results.

2. Calculation Details

Configurations of the liquid were generated by classical MC simulations that were then used in subsequent QM calculations. In this section we first describe the details of the MC simulation. Next we discuss how we sample configurations for the QM calculations and the procedures used for including polarization. Finally we discuss the QM models in the calculations of the NMR parameters.

The MC simulations were performed using the DICE program¹⁹ in the isothermal–isobaric, NPT, ensemble with 500 ammonia molecules. We have considered $P = 1$ atm and $T =$

197.2 K. Intermolecular interactions were modeled by the standard Lennard–Jones (LJ) plus Coulomb potential with three parameters for each interacting site. The atomic charges used for ammonia were updated to account for the polarization in the liquid state and are described later in this section. For the LJ potential we have selected two different potentials to clarify the role played by the choice of the classical potential. The first is due to Impey and Klein²⁰ and the other is due to Gao, Xia, and George.²¹ We will now refer to the IK and GXG models, respectively. Initially the atomic charges were obtained using an electrostatic potential fit using the results of MP2/aug-cc-pVTZ gas-phase calculation. The ammonia geometry was initially optimized in the gas-phase using this same MP2/aug-cc-pVTZ level of calculation.

An important aspect in the classical simulation is the proper treatment of the electronic polarization in the liquid phase. Solute polarization is the change in the electrostatic moments of a reference molecules due to the electric field of the solvent molecules. This is then a solvent-dependent result and needs consideration for each specific environment. This has been a persistent concern that has seen several interesting procedures.²² Because NMR parameters are local properties and depend on the electronic distribution around every nucleus, the relaxation of the electrostatic moments due to the solute polarization is expected to have important consequences in the NMR properties. The spin coupling and the chemical shielding should be affected differently. Thus, it is very important to have a systematic investigation of the effects of the solute polarization. In this work we have used an iterative procedure previously developed.²³ When the structures generated by the MC simulations are used, an average solvent electrostatic configuration (ASEC)²⁴ is produced and MP2/aug-cc-pVTZ calculations are made to obtain the atomic charges by fitting an electrostatic potential in a grid (CHELPG).²⁵ Another simulation is performed with these new atomic charges, a new sampling is made generating another ASEC, and another MP2/aug-cc-pVTZ calculation is performed to obtain the new values of the atomic charges. This procedure is repeated until convergence is achieved. The convergence is tested on the dipole moment. Normally we find sufficient a convergence criterion of $\Delta\mu \leq 0.1$ D. But to analyze the role of the polarization on the NMR properties we have used a total of 10 cycles. For constructing the ASEC we have used 400 configurations with 13–15% of statistical correlation and each configuration is composed of a total of 260 ammonia molecules (corresponding to a radius of 12.3 Å), treated as point charges. Within the iteration we used two options, allowing for the geometry relaxation or using a fixed geometry. In the first option, after each MC simulation (along which the molecules are kept rigid) both the geometry and the charge distribution of ammonia are relaxed by using the MP2/aug-cc-pVTZ gradient calculated in the presence of the ensemble averaged solvent electric field represented by point charges. The updated geometry and charge distribution is then used in the next MC simulation. This protocol is based on the Free Energy Gradient method.²⁶ In the second option the ammonia geometry was kept fixed in the gas-phase arrangement and only the charge distribution was relaxed. The MP2/aug-cc-pVTZ level gives very accurate geometry, electric dipole moment, and dipole polarizability for the ammonia molecule in gas phase and is therefore suitable for our study. Note that the classical force field is not used to relax the geometry but, instead, a MP2/aug-cc-pVTZ gradient calculation. The same is used to relax the atomic charges. The force field is used only during the MC simulations, in which all the molecules are rigid.

Both the relaxed-geometry and fixed-geometry calculations are made using the MC simulations performed for the two force fields (differing only in the LJ parameters as mentioned before, while the coulomb term is the same and is calculated systematically). The two force fields, IK and GXG, give significantly different bulk properties (like densities) and one of our purposes was to observe whether the local properties of ammonia that we want to investigate (magnetic shielding and SSCC) in liquid environment are significantly affected or not by the LJ parameters. As we shall see, we observed that geometry (in the relaxed case) and electric dipole moment are little affected by the change in the LJ parameters. As we have used 10 iterations, considering the two force fields and the two ammonia geometries (rigid and relaxed) a total of 40 MC simulations were made. Typically, each simulation consisted of 40×10^7 MC steps. To analyze the role of the solute polarization we calculate the NMR parameters in every step of the iterative procedure. This will give a good picture on how these NMR parameters depend on the electrostatic polarization obtained in the liquid phase. Another alternative also analyzed here is to consider the problem of one solute NH_3 molecule in the environment of the other NH_3 solvent molecules. As such, in the polarization scheme we only update the electrostatic moment of the solute. In this case we will refer to central polarization in contrast to the full polarization, where the charges of all NH_3 molecules are updated.

The QM calculation of the magnetic properties of ammonia were made using the density functional theory with the B3LYP exchange correlation.²⁷ The basis sets used were specially designed for the calculation of NMR parameters. For the coupling constants two basis sets were used. The first is the one developed by Provasi et al.^{28,29} and is termed aug-cc-pVTZ-J. The other is due to Jensen³⁰ and is termed aug-pcJ-2. For the calculations of the magnetic shielding, we have used the aug-pcS-3.³¹ All QM calculations were performed using the GAUSSIAN 03 program.³² The selection of the exchange functional for NMR calculations has to be made with some care.⁶⁶ Our choice for B3LYP is based on the recent study of Keal et al.^{6h} that indicates a very good performance for the spin coupling of ammonia.

The theory of the nuclear magnetic shielding,³³ the SSCC³⁴ and the different computational methods for calculating them have been extensively described in the literature.³⁵ However, we can mention that the four Ramsey's contributions to the SSCC are: (i) the Fermi contact (FC); (ii) the spin-dipolar (SD), that accounts for the interaction of the nuclear magnetic moments with the spin of the electrons; (iii) the diamagnetic spin orbital (DSO); and (iv) the paramagnetic spin orbital (PSO), which account for the interaction of the nuclear spins with the orbital angular momentum of the electrons. For completeness we report these individual contributions and compare the total value with the experimental results.

3. Results and Discussions

3.1. Solute Polarization. Table 1 gives the MP2/aug-cc-pVTZ results for the average dipole moment of ammonia using the different models considered. The calculated gas phase result is 1.562 D, in very good agreement with the experimental result of 1.56 D.³⁶ The solute polarization considerably increases the in-liquid dipole moment and the increased value depends on the model used. For instance, using the IK model²⁰ with full polarization and geometry relaxation one obtains the dipole moment of liquid ammonia as 2.30 D, corresponding to an increase of about 50%. But different models give slightly

TABLE 1: MP2/aug-cc-pVTZ Results for the Dipole Moment (*D*) of Liquid Ammonia^a

model	dipole moment (<i>D</i>)
Full Polarization	
GXG rigid	2.33
GXG relaxed	2.51
IK rigid	2.24
IK relaxed	2.30
Central Polarization	
GXG rigid	1.97
IK rigid	1.92
previous estimates ³⁷	$2.05 \pm 0.09, 2.02 \pm 0.10$

^a The calculated values are obtained with the average solvent electrostatic configuration formed from 400 statistically uncorrelated configurations obtained from MC simulation. See text.

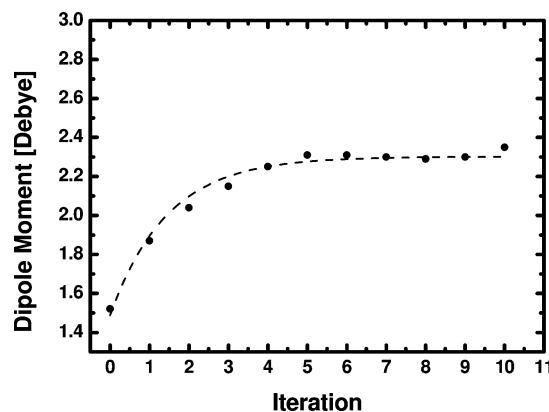


Figure 1. Evolution of the MP2/aug-cc-pVTZ results for the dipole moment of in-liquid ammonia with respect to the number of iterations for obtaining the liquid polarization.

different results. When the central solute molecule is polarized alone in the field of all the remaining solvent molecules the calculated dipole moments are 1.92 and 1.97 D for the IK and GXG models, respectively. These results could be compared with a previous estimate³⁷ of 2.05 ± 0.10 D for the dipole moment of liquid ammonia. In these cases one obtains from the NPT MC simulation the calculated densities of 0.634 and 0.653 g/cm^3 in comparison with experimental result of 0.731 g/cm^3 . We find evidence that the full polarization has a tendency to give increased liquid densities. For instance, with the rigid GXG model the calculated density is 0.884 g/cm^3 . It is seen in Table 1 that using the full polarization increases the in-liquid dipole moment and it increases even further with geometry relaxation. The in-liquid bond length and bond angle are obtained as $R_{(\text{N-H})} = 1.017 \pm 0.002 \text{ \AA}$, $\Theta_{(\text{H-N-H})} = 105 \pm 1^\circ$. As the calculated gas phase result is 1.012 Å and 106.8° this corresponds to an increase of 0.005 Å in the bond length and a decrease of the angle $\Theta_{(\text{H-N-H})}$ of about 2° , corresponding then to a slight increase of the pyramidality of NH_3 . For illustration, Figure 1 shows the iterative results for the dipole moment of liquid ammonia using the IK model with geometry relaxation. The influence of the electrostatic polarization on the calculated NMR parameters is analyzed in the next sections.

3.2. Intramolecular Indirect Spin-Spin Coupling Constant. The values of the $^1J(\text{N-H})$ and $^2J(\text{H-H})$ couplings in the liquid case are shown in Table 2 and in Figures 2 and 3. In both cases we observe that the FC contribution dominates the total intramolecular couplings in ammonia. Thus the accurate determination of FC is crucial for obtaining reliable results for the coupling constants. The two-bond $^2J(\text{H-H})$ coupling

TABLE 2: Total and the Separate Contributions to the Intramolecular Spin–Spin Coupling (in Hz) Calculated with the B3LYP/aug-cc-pVTZ-J Level of Approximation and Corresponding to the Full Polarization and Relaxation^a

coupling	model	total	FC	SD	PSO	DSO	
¹ J(N–H)	gas phase	–64.37					
			liquid	–60.96	–0.24	–3.10	–0.07
	GXG rigid	–67.77 (–66.31)	–64.65	–0.14	–2.91	–0.07	
	GXG relaxed	–64.35 (–63.41)	–61.26	–0.10	–2.92	–0.06	
	IK rigid	–67.31	–64.14	–0.16	–2.94	–0.07	
	IK relaxed	–63.92	–60.75	–0.13	–2.98	–0.06	
	exp.	–61.2 ± 0.3; ^c –61.2 ± 0.9; ^d –61.45 ± 0.2 ^e					
² J(H–H)	exp., vib. avg. ^b	–61.6; –61.6; –61.9					
	gas phase	–10.32	–11.82	0.60	6.15	–5.25	
			liquid				
	GXG rigid	–11.49	–12.80	0.60	6.01	–5.30	
	GXG relaxed	–13.01	–14.32	0.65	5.63	–4.96	
	IK rigid	–11.30	–12.64	0.60	6.03	–5.29	
	IK relaxed	–12.56	–13.93	0.65	5.73	–5.01	
	exp.	–10.35 ± 0.8; ^d –9.6 ± 0.2 ^e					
	exp.; vib. avg. ^b	–11.1; –10.3					

^a The calculated geometries are $R_{(N-H)} = 1.017 \pm 0.002$ Å, $\Theta_{(H-N-H)} = 105 \pm 1^\circ$ for relaxed NH₃ and $R_{(N-H)} = 1.012$ Å, $\Theta_{(H-N-H)} = 107.10$ for rigid NH₃. Estimated statistical error is 0.20 Hz. In parentheses are shown the corresponding values including the hydrogen-bonded molecules explicitly. See text. ^b The experimental value after correcting for the zero-point vibration. See ref 15g. ^c Ref 11. ^d Ref 12. ^e Ref 13.

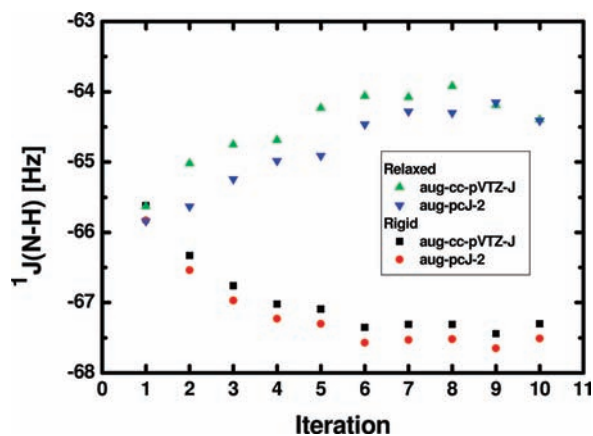


Figure 2. Evolution of the total ¹J(N,H) [in Hz] with the enhancement of the solute polarization for the Impey-Klein model with rigid and relaxed geometries using aug-cc-pVTZ-J and aug-pcJ-2 basis sets.

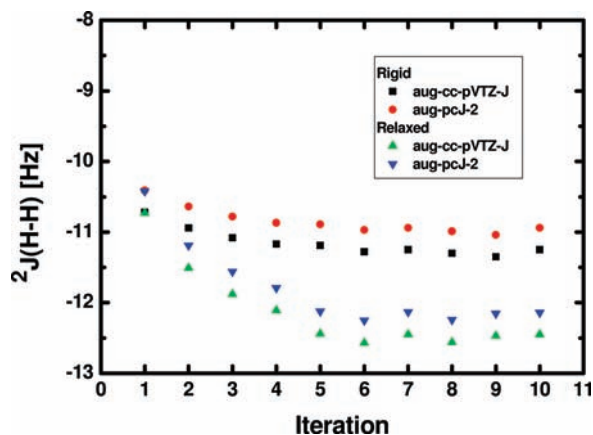


Figure 3. Evolution of the total ²J(H,H) [in Hz] with the enhancement of the solute polarization for the Impey-Klein model with rigid and relaxed geometries using aug-cc-pVTZ-J and aug-pcJ-2 basis sets.

constant presents relatively high PSO and DSO contributions, but these have opposite signs so that they almost cancel each other.

The experimental intramolecular couplings are also shown in Table 2, including the estimate of their vibration corrected

values obtained by subtracting the zero-point vibration correction, as previously calculated by Ruden et al.^{15g} Comparing the results obtained with both force field models used to the most recent experiments made by Wasylishen and Friedrich¹³ we find that the calculations slightly overestimate the coupling constant strengths. For instance, using the IK model with geometry relaxation leads to the value of –63.9 Hz compared to the experimental value of –61.9 Hz. These differences are small and have the value of 2.47 Hz for ¹J(N–H) with the IK model and 2.92 Hz with the GXG model. For ²J(H–H) the difference is 2.96 Hz with the IK model and 3.41 Hz with GXG model. As seen previously, the zero-point vibration correction reduces these differences in 0.4 Hz for the ¹J(N–H) coupling and 0.7 Hz for the ²J(H–H) coupling. We also note from Table 2 that inclusion of geometry relaxation affects the spin couplings differently. It decreases (in module) the strength of the ¹J(N–H) coupling and increases the strength of the ²J(H–H) coupling. The ASEC procedure used here only includes the average electrostatic part. As ammonia is a well structured liquid with relatively strong hydrogen bonds it is important to consider some solvent molecules explicitly. We have identified and separated all contributions that make a hydrogen bond with a selected ammonia treated as reference molecule. The hydrogen bonds are identified using the geometric and energetic criteria discussed several times before.³⁸ These include all hydrogen bonds, whether the NH₃ is considered a donor or an acceptor of it. For obtaining the ¹J(N–H) coupling for this case we have embedded these hydrogen bonded molecules in the electrostatic field of the remaining. The results are also shown in Table 2 for the GXG model. Hydrogen bonds thus have some effect on the calculated coupling reducing its value compared to the electrostatic-only result. However, the change is found to be small, reducing the ¹J(N–H) by about 1.0–1.5 Hz but in the correct direction compared to the experimental value.

Figures 2 and 3 summarize the dependence of the calculated spin–spin coupling constants on the electrostatic polarization experienced by ammonia in the liquid phase and on the consequent geometry relaxation. The main effect observed in the variation of the ¹J(N,H) coupling constant with the polarization, Figure 2, is that for a rigid geometry it decreases with the increase of the polarization, whereas the relaxed geometry shows

TABLE 3: Separate Contributions to the Total Solvent Effect on the Spin–Spin Coupling Constants^a

contribution	coupling	IK model	GXG model
PSE	$\Delta^1J(\text{N–H})_{\text{vapor–liquid}}$	–2.9	–3.4
	$\Delta^2J(\text{H–H})_{\text{vapor–liquid}}$	–1.0	–1.2
PGE	$\Delta^1J(\text{N–H})_{\text{rigid–relaxed}}$	3.4	3.4
	$\Delta^2J(\text{H–H})_{\text{rigid–relaxed}}$	–1.3	–1.5
total	$\Delta^1J(\text{N–H})$	0.5	0.0
	$\Delta^2J(\text{H–H})$	–2.3	–2.7

^aPure (unrelaxed) solvent contribution (PSE) and geometrical effect (PGE) are shown separately. Results obtained with the IK and GXG models and the B3LYP/aug-cc-pVTZ-J level of approximation. See text and Table 1.

an equivalent increase. The variation of the $^2J(\text{H,H})$ coupling with the solute polarization is shown in Figure 3. We note that the difference in the calculated coupling constants using either basis set is less than 0.3 Hz. We also note that the full and central polarization alternatives have little effect on the spin coupling constants. For instance, polarizing only the central molecule the GXG model gives –66.42 Hz for the $^1J(\text{N–H})$ constant and –10.61 Hz for the $^2J(\text{H–H})$ constant. These values differ little from those reported in Table 2.

The results of Table 2 show that the $^1J(\text{N,H})$ coupling constant in the liquid phase is essentially the same as in vapor. There is essentially no solvent shift when this coupling constant is calculated in the liquid and in the isolated vapor form. This is consistent with the experiments that could not detect any solvent shift in the liquid–vapor change.^{11,12,16b,17b} It is convenient to consider that theoretically the solvent effects to the calculated couplings constants can be separated into two parts. So we analyze separately the solvent effects without consideration of the geometry relaxation and the influence of the change in geometry in the liquid phase. These are shown in Table 3 where the pure solvent effect is obtained using the results for the rigid geometry. For the $^1J(\text{N,H})$ constant with the IK model we obtain a contribution of –2.9 Hz. This is then essentially canceled by the additional contribution of the geometry relaxation (3.4 Hz), which leads to the total result of only 0.5 Hz for the total shift of $^1J(\text{N,H})$ in the liquid phase compared to the value in vapor. We also note that the two potential models adopted here give essentially the same qualitative and quantitative results. Thus, although the calculation of $^1J(\text{N,H})$ does not completely agree with experiment, the liquid–vapor shift is very well predicted. It is also important to notice that the results obtained for $^1J(\text{N,H})$ with the relaxed geometry are better than with the rigid one.

For the $^2J(\text{H,H})$ constant we obtain a total shift of about –2.5 Hz. Contreras and Peralta³⁹ have previously studied pure geometrical effects of several spin–spin coupling constants. For ammonia, in particular, they reported a decrease of the $^1J(\text{N,H})$ and an increase of the $^2J(\text{H,H})$ constant when the pyramidal angle increases. This is in due agreement with our present findings. Considering that the change from the gas to the liquid phase changes the angle $\Theta_{(\text{H–N–H})}$ in 2.2° toward a higher pyramidal angle and considering also that the reference angle of 106.5° used by Contreras and Peralta³⁹ is very close to the angle of 107.1° obtained here we can also obtain the geometrical effects from eqs 9 and 32 of ref 39. Thus, the pure geometrical effects corresponding to the gas-to-liquid transition are 4.4 Hz for $^1J(\text{N,H})$ and –1.7 Hz for $^2J(\text{H,H})$. These can be compared to our explicit values of 3.4 and –1.5 Hz, respectively.

From Table 3 we can see that both models with relaxed geometries predict that the difference between gas and liquid

phase of $^1J(\text{N–H})$ is about 0.5 Hz or less, whereas the same difference in $^2J(\text{H,H})$ is about –2.5 Hz. Of course, the $^2J(\text{H,H})$ coupling can not be measured directly because of the chemical and magnetic equivalence of the three protons but there is an available experimental result derived from partially deuterated ammonia,¹¹ that is used here as a guide to our numerical results.

3.3. Chemical Shielding. Now we turn to the discussion of the chemical shielding $\sigma(^{15}\text{N})$. The chemical shielding in the liquid phase at $T = 195.5$ K has been determined experimentally¹² to be 264.3 ppm. This corresponds to a chemical shift of –22.6 ppm in comparison to the result in the vapor.¹² Several complementary theoretical models have been used here to establish the qualitative contributions of electrostatic, solute–solvent hydrogen bonds, and van der Waals terms.⁴ The electrostatic term can be determined by simply considering the reference molecule embedded in the electrostatic field of the remaining ones. In this case a single NH_3 molecule is surrounded by all the others treated as simple point charges. We have thus included all remaining NH_3 molecules up to a distance of 12.25 Å, corresponding to 260 NH_3 molecules. As explained before, we have used these to obtain the ASEC configuration. For this case different polarizations have been used. The first one simply uses the calculated gas phase charges. Next, we have used a partial polarization corresponding to iteration 2 in Figure 1 because it leads to a dipole moment of 2.02 D as in the previous estimate.³⁶ Finally we have used the fully converged polarization obtained here, corresponding to a larger dipole moment of 2.3 D. For the calculation of the hydrogen bond contribution we have used the same procedure used previously for the spin coupling parameters. Again, for obtaining the chemical shielding for this case we have embedded these hydrogen bonded molecules in the electrostatic field of the remaining. As we will see below explicitly including hydrogen bonded ammonia molecules is essential for obtaining the proper vapor–liquid chemical shift. Finally, for adding more of the van der Waals and the bulk contribution we have explicitly included all NH_3 molecules within the first solvation shell. This corresponds to 12 explicit NH_3 molecules surrounded by the remaining 248 molecules treated as point charges.

Because the small relaxation of the NH_3 is found to have little effect on the calculated shifts Table 4 only shows the results using the rigid GXG model. The gas phase value corresponding to vapor measurements is also calculated using the B3LYP/aug-cc-pcS-3 level of approximation and the result obtained is 259.9 ppm in good agreement with the experimental value¹² of 264.3 ppm. The calculated chemical shifts are also shown and allow a systematic analysis of the different contributions. We find here that the electrostatic contribution alone is not sufficient for a proper description of the chemical shift. In fact, as it can be seen in Table 4 the electrostatic contribution alone gives a shift in the wrong direction. Table 4 also shows that this is also the case in the polarizable continuum model (PCM).⁴⁰ However, after including the explicitly hydrogen bonded NH_3 molecules the correct sign is obtained for the chemical shift. The value obtained in this case is now –28.0 ppm in good agreement with experiment. The explicit use of hydrogen bonded molecules includes the van der Waals interaction with the closest solvent molecules. Additional inclusion of more solvent molecules in this case overshoots the experimental value. It is clear that the inclusion of explicit solvent molecules is very important for a proper qualitative understanding of the chemical shift of $\sigma(^{15}\text{N})$ in liquid ammonia. However, the use of the entire solvation shell of explicit molecules leads to results that are larger than experiments, perhaps a consequence of an overestimated

TABLE 4: Nuclear Magnetic Shielding, $\sigma(^{15}\text{N})$, and Vapor to Liquid Shift, $\Delta\sigma(^{15}\text{N})$ (in ppm) Obtained with the B3LYP/ aug-pcS-3 Level of Approximation and Corresponding to the Polarization in the Rigid GXG Model (See Text)

	gas		liquid				liquid	
	calcd	measured ^a	partial polariz. PC ^b	PCM ^c	full polariz. PC ^d	HB + PC ^e	1st shell + PC ^f	measured ^a
$\sigma(^{15}\text{N})$	259.9	264.3	263.9	262.9	266.8	231.9 (245.9)	220.8 (234.7)	241.7
$\Delta\sigma(^{15}\text{N})$			+4.0	+3.0	+6.9	-28.0 \pm 1.2 (-14.0 \pm 1.0)	-39.1 \pm 0.6 (-25.2 \pm 1.0)	-22.6

^a Experimental results of ref 12 obtained at $T = 195.5$ K. ^b Electrostatic embedding only (PC stands for point charges) with partial polarization corresponding to iteration 2 in Figure 1. In-liquid dipole moment is 2.02 D. ^c Polarizable continuum model. In-liquid dipole moment is 1.90 D. ^d Electrostatic embedding only (PC stands for point charges) with full polarization. In-liquid dipole moment is 2.33 D. ^e Includes explicit hydrogen bonded molecules in the electrostatic embedding of the remaining NH₃ molecules. Value in parentheses is obtained with the central polarization. In-liquid dipole moment is 1.97 D. ^f Includes explicitly 12 NH₃ molecules in the electrostatic embedding of the remaining NH₃ molecules. Value in parentheses below is obtained with the central polarization.

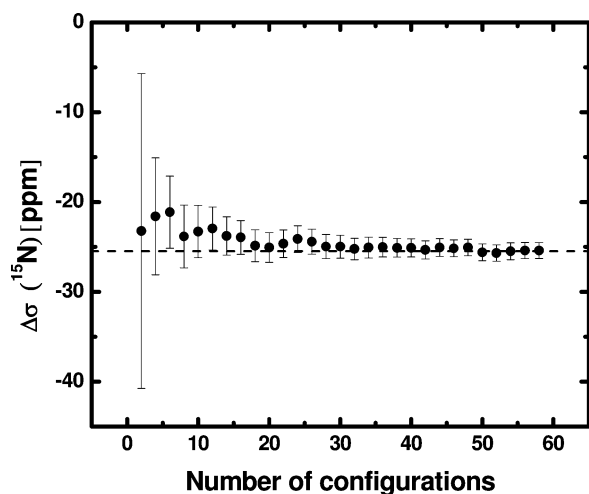


Figure 4. Calculated $\Delta\sigma(^{15}\text{N})$ as a function of the number of statistically uncorrelated configurations used. Note the fast convergence of the average value. Uncertainty is the statistical error.

polarization. This is corroborated by the results obtained with the central polarization where a more realistic liquid density is obtained (section 3.1). In this case the chemical shift is calculated as -25.2 ppm in good agreement with experiment.

The effect of moving from a central to a full polarization approach is larger in the HB + PC and first shell + PC schemes than in the PC scheme. This is because the polarization effect on the shielding expresses itself through a change of the intermolecular distances and relative orientations rather than of the average solvent electrostatic configuration.

An important aspect of liquid simulation studies is to ensure statistically converged results. Figure 4 shows for illustration the convergence of the calculated chemical shift $\Delta\sigma(^{15}\text{N})$. The fast convergence is a consequence of the use of statistically uncorrelated configurations.¹⁸

4. Summary and Conclusions

The theoretical challenge of obtaining nuclear magnetic resonance properties of molecular liquids is addressed. The $^1J(\text{N,H})$ and $^2J(\text{H,H})$ intramolecular spin–spin coupling constants and the $\sigma(^{15}\text{N})$ chemical shielding of liquid ammonia have been studied using the sequential QM/MM method. Monte Carlo simulations are made to generate liquid structures for subsequent quantum mechanical calculations using density functional theory. Specific basis sets are used for each NMR property. Electronic polarization is included and its influence on the calculated properties has been considered. Two intermolecular potentials are used. The calculated results for the $^2J(\text{H,H})$ coupling constant vary from -10.6 to -13.01 Hz depending on the theoretical model used. These are in good agreement

with the experimental results. For $^1J(\text{N,H})$ the results vary between -67.8 and -63.9 Hz, in comparison with the experimental value of -61.5 Hz. The vapor to liquid shift is calculated as about -2.5 Hz (unfortunately, there is no experimental value for comparison) for $^2J(\text{H,H})$ and is essentially null (calculated here as -0.5 Hz) for the $^1J(\text{N,H})$ parameter. This is in agreement with experiment where the vapor to liquid shift of $^1J(\text{N,H})$ has been found to be less than 0.8 Hz. An analysis of the theoretical results suggest that the shift is canceled by equivalent and opposite contributions of the pure solvent and geometry relaxation contributions. For the chemical shielding we find that the vapor to liquid chemical shift requires the explicit use of solvent molecules. Considering only one ammonia molecule in an electrostatic embedding gives a wrong sign for the chemical shift that is corrected only with the use of explicit and additional molecules. The present results for liquid NH₃ confirm that the chemical shielding is more sensitive to the electronic polarization than the spin–spin coupling constant.

Acknowledgment. R.M.G., H.C.G., and S.C. acknowledge financial support from CNPq, CAPES, and FAPESP (Brazil). M.C.C. acknowledges financial support from the University of Buenos Aires (UBACYT, X-035). P.F.P. acknowledges financial support from CONICET, ANPCyT, and UNNE (FONCYT, PICTO-UNNE-227, BID-1728/OC-AR). We thank CENAPAD for computational support.

References and Notes

- (1) Hore, P. J. *Nuclear Magnetic Resonance*; Oxford University Press: New York, 1995.
- (2) Mennucci, B.; Cammi, R., Eds. In *Continuum Solvation Models in Chemical Physics*; Wiley: New York, 2007.
- (3) Canuto, S., Ed. In *Solvation Effects on Molecules and Biomolecules. Computational Methods and Applications*; Springer: New York, 2008.
- (4) Buckingham, A. D.; Schafer, T.; Schneider, W. G. *J. Chem. Phys.* **1960**, *32*, 1227.
- (5) (a) Mennucci, B.; Martinez, J. M.; Tomasi, J. *J. Phys. Chem. A* **2001**, *105*, 7287. (b) Mennucci, B. *J. Am. Chem. Soc.* **2002**, *124*, 1506. (c) Kongsted, J.; Mennucci, B. *J. Phys. Chem. A* **2007**, *111*, 9890.
- (6) (a) Malkin, V. G.; Malkina, O. L.; Steinebrunner, G.; Huber, H. *Chem.–Eur. J* **1996**, *2*, 452. (b) Chesnut, D. B.; Rusiloski, B. E. *J. Mol. Struct.* **1994**, *314*, 19. (c) Cheeseman, J. R.; Trucks, G. W.; Keith, T. A.; Frisch, M. J. *J. Chem. Phys.* **1996**, *104*, 5497. (d) Fileti, E. E.; Georg, H. C.; Coutinho, K.; Canuto, S. *J. Braz. Chem. Soc.* **2007**, *18*, 74. (e) Kongsted, J.; Aidas, K.; Mikkelsen, K. V.; Sauer, S. P. A. *J. Chem. Theory Comput.* **2008**, *4*, 267. (f) Møgelhøj, A.; Aidas, K.; Mikkelsen, K. V.; Sauer, S. P. A.; Kongsted, J. *J. Chem. Phys.* **2009**, *130*, 134508. (g) Ligabue, A.; Sauer, S. P. A.; Lazzarotti, P. *J. Chem. Phys.* **2007**, *126*, 154111. (h) Keal, T. W.; Helgaker, T.; Salek, P.; Tozer, D. *J. Chem. Phys. Lett.* **2006**, *425*, 163.
- (7) Onsager, L. *J. Am. Chem. Soc.* **1936**, *58*, 1486.
- (8) Kirkwood, J. G. *J. Chem. Phys.* **1934**, *2*, 351.
- (9) Fonseca, T. L.; Coutinho, K.; Canuto, S. *J. Chem. Phys.* **2008**, *129*, 034502.
- (10) (a) Witanoswski, M.; Sicinska, W.; Biernat, S. *J. Magn. Reson.* **1991**, *91*, 289. (b) Witanoswski, M.; Stefaniak, L.; Webb, G. A. In *Annual Reports on NMR Spectroscopy*; Webb, G. A., Ed.; Academic Press: London, 1993; vol. 25.

- (11) Bernheim, R. A.; Batiz-Hernandez, H. *J. Chem. Phys.* **1964**, *40*, 3446.
- (12) Alei, M., Jr.; Florin, A. E.; Litchman, W. M.; O'Brien, J. F. *J. Phys. Chem.* **1971**, *75*, 932.
- (13) Wasylshen, R. E.; Friedrich, J. O. *Can. J. Chem.* **1987**, *65*, 2238.
- (14) Berthier, C.; Berthier, G. *Theor. Chim. Acta* **1969**, *14*, 71.
- (15) (a) Hinchliffe, A.; Cook, D. B. *Theor. Chim. Acta* **1970**, *17*, 91. (b) Galasso, V. *Theor. Chim. Acta* **1983**, *63*, 35. (c) Perera, S. A.; Sekino, H.; Bartlett, R. J. *J. Chem. Phys.* **1994**, *101*, 2186. (d) Jackowski, K.; Barszczewicz, A. *J. Mol. Struct.: THEOCHEM* **1998**, *434*, 47. (e) Lantto, P.; Vaara, J. *J. Chem. Phys.* **2001**, *114*, 5482. (f) Janowski, T.; Jaszufski, M. *Int. J. Quantum Chem.* **2002**, *90*, 1083. (g) Ruden, T. A.; Lutmaes, O. B.; Helgaker, T.; Ruud, K. *J. Chem. Phys.* **2003**, *118*, 9572. (h) Pecul, M.; Sadlej, J.; Helgaker, T. *Chem. Phys. Lett.* **2003**, *372*, 476. (i) Keal, T. W.; Helgaker, T.; Salek, P.; Tozer, D. J. *Chem. Phys. Lett.* **2006**, *425*, 163. (j) Alkorta, I.; Provasi, P. F.; Aucar, G. A.; Elguero, J. *Magn. Reson. Chem.* **2007**, *46*, 356.
- (16) (a) Litchman, W. M.; Alei, M., Jr.; Florin, A. E. *J. Chem. Phys.* **1969**, *50*, 1031. (b) Litchman, W. M.; Alei, M., Jr.; Florin, A. E. *J. Chem. Phys.* **1969**, *50*, 1897.
- (17) (a) Jameson, C. J.; Jameson, A. K.; Oppusunggu, D.; Wille, S.; Burrell, P. M.; Mason, J. *J. Chem. Phys.* **1981**, *74*, 81. (b) Jameson, C. J.; Jameson, A. K.; Cohen, S. M.; Parker, H.; Oppusunggu, D.; Burrell, P. M.; Wille, S. *J. Chem. Phys.* **1981**, *74*, 1608.
- (18) (a) Coutinho, K.; Canuto, S. *J. Chem. Phys.* **2000**, *113*, 9132. (b) Coutinho, K.; Canuto, S.; Zerner, M. C. *J. Chem. Phys.* **2000**, *112*, 9874. (c) Canuto, S.; Coutinho, K.; Trziesniak, D. *Adv. Quantum Chem.* **2003**, *41*, 161.
- (19) Coutinho K.; Canuto, S. *DICE, a Monte Carlo program for molecular liquid simulations*; University of São Paulo: São Paulo, Brazil, 2003.
- (20) Impey, R. W.; Klein, M. L. *Chem. Phys. Lett.* **1984**, *104*, 579.
- (21) Gao, J.; Xia, X.; George, T. F. *J. Phys. Chem.* **1993**, *97*, 9241.
- (22) (a) Georg, H. C.; Coutinho, K.; Canuto, S. *J. Chem. Phys.* **2007**, *126*, 034507. (b) Coutinho, K.; Canuto, S. *Adv. Quantum Chem.* **1997**, *28*, 89. (c) Coutinho, K.; Canuto, S. *J. Chem. Phys.* **2000**, *113*, 9132. (d) Ludwig, V.; Coutinho, K.; Canuto, S. *Phys. Chem. Chem. Phys.* **2007**, *9*, 4907. (e) Jorgensen, W. L. *J. Chem. Theory. Comput.* **2007**, *3* (special issue no. 6), 1877–2145. (f) Cramer, C. J.; Truhlar, D. G. *Science* **1992**, *256*, 213. (g) Kongsted, J.; Osted, A.; Mikkelsen, K. V.; Christiansen, O. *Chem. Phys. Lett.* **2002**, *364*, 379. (h) Wallqvist, A.; Ahlström, P.; Karlström, G. *J. Phys. Chem.* **1990**, *94*, 1649. (i) McDonald, N. A.; Carlson, H. A.; Jorgensen, W. L. *J. Phys. Org. Chem.* **1997**, *10*, 563. (j) Warshell, A.; Kato, M.; Pisljakov, A. V. *J. Chem. Theor. Comput.* **2007**, *3*, 2034. (k) Martin, M. E.; Sánchez, M. L.; Oliveira del Valle, F. J.; Aguilar, M. A. *J. Chem. Phys.* **2000**, *113*, 6308. (l) Coutinho, K.; Georg, H. C.; Fonseca, T. L.; Ludwig, V.; Canuto, S. *Chem. Phys. Lett.* **2007**, *437*, 148. (m) Sánchez, M. L.; Aguilar, M. A.; Olivares Del Valle, F. J. *J. Comput. Chem.* **1997**, *18*, 313. (n) Gao, J.; Luque, F. J.; Orozco, M. *J. Chem. Phys.* **1993**, *98*, 2975.
- (23) Georg, H. C.; Coutinho, K.; Canuto, S. *Chem. Phys. Lett.* **2006**, *429*, 119.
- (24) Coutinho, K.; Georg, H. C.; Fonseca, T. L.; Ludwig, V.; Canuto, S. *Chem. Phys. Lett.* **2007**, *437*, 148.
- (25) Breneman, C. M.; Wiberg, K. B. *J. Comput. Chem.* **1990**, *11*, 361.
- (26) (a) Hirao, H.; Nagaoka, Y.; Nagaoka, M. *Chem. Phys. Lett.* **2001**, *348*, 350. (b) Okuyama Yoshida, N.; Kataoka, K.; Nagaoka, M.; Yamabe, T. *J. Chem. Phys.* **2000**, *113*, 3519. (c) Okuyama-Yoshida, N.; Nagaoka, M.; Yamabe, T. *Int. J. Quantum Chem.* **1998**, *70*, 95. (d) Fdez. Galván, I.; Sánchez, M. L.; Martín, M. E.; Olivares del Vale, F. J.; Aguilar, M. A. *J. Chem. Phys.* **2003**, *118*, 255.
- (27) (a) Becke, A. D. *J. Chem. Phys.* **1993**, *98*, 5648. (b) Lee, C.; Yang, W.; Parr, R. G. *Phys. Rev. B* **1988**, *37*, 785.
- (28) Provasi, P. F.; Aucar, G. A.; Sauer, S. P. A. *J. Chem. Phys.* **2001**, *115*, 1324.
- (29) The aug-cc-pVTZ-J basis sets can be downloaded from <https://bse.pnl.gov/bse/portal>.
- (30) Jensen, F. *J. Chem. Theory Comput.* **2006**, *2*, 1360.
- (31) Jensen, F. *J. Chem. Theory Comput.* **2008**, *4*, 719.
- (32) Frisch, M. J.; . *Gaussian 03*, Revision D.02; Gaussian, Inc.: Wallingford, CT, 2004.
- (33) Ramsey, N. F. *Phys. Rev.* **1950**, *78*, 699.
- (34) Ramsey, N. F. *Phys. Rev.* **1953**, *91*, 303.
- (35) (a) Helgaker, T.; Jaszufski, M.; Ruud, K. *Chem. Rev.* **1999**, *99*, 293. (b) Sauer, S. P. A.; Packer, M. J.; John Wiley and Sons: London, 2000. (c) Krivdin, L. B.; Contreras, R. H. *Annu. Rep. NMR Spectrosc.* **2007**, *61*, 133. (d) Vaara, J. *Phys. Chem. Chem. Phys.* **2007**, *9*, 5399. (e) Helgaker, T.; Jaszufski, M.; Pecul, M. *Prog. Nucl. Magn. Reson. Spectrosc.* **2008**, *53*, 249. (f) Fukui, H. *Prog. Nucl. Magn. Reson. Spectrosc.* **1997**, *31*, 317. (g) Oddershede, J. *Adv. Quantum Chem.* **1978**, *11*, 275. (h) Geertsen, J.; Eriksen, S.; Oddershede, J. *Adv. Quantum Chem.* **1991**, *22*, 167.
- (36) Marshall, M. D.; Igzi, K. C.; Muentner, J. S. *J. Chem. Phys.* **1997**, *107*, 1035.
- (37) Almeida, T. S.; Coutinho, K.; Cabral, B. J. C.; Canuto, S. *J. Chem. Phys.* **2008**, *128*, 014506.
- (38) (a) Malaspina, T.; Coutinho, K.; Canuto, S. *J. Chem. Phys.* **2002**, *117*, 1692. (b) Fileti, E. E.; Coutinho, K.; Malaspina, T.; Canuto, S. *Phys. Rev. E* **2003**, *67*, 61504.
- (39) Contreras, R. H.; Peralta, J. E. *Prog. Nucl. Magn. Reson. Spectrosc.* **2000**, *37*, 321.
- (40) Miertus, S.; Scrocco, E.; Tomasi, J. *Chem. Phys.* **1981**, *55*, 117.